

HERG-like K⁺ Channels in Microglia

WEI ZHOU,* FRANCISCO S. CAYABYAB,†§ PETER S. PENNEFATHER,†§|| LYANNE C. SCHLICHTER,†§
and THOMAS E. DECOURSEY*

From the *Department of Molecular Biophysics and Physiology, Rush Presbyterian St. Luke's Medical Center, Chicago, Illinois 60612; †Playfair Neuroscience Unit, Toronto Hospital Research Institute, Toronto, Ontario M5T 2S8, Canada; ‡Department of Physiology, University of Toronto, Toronto, Ontario M5S 1A1, Canada; and ||Faculty of Pharmacy, University of Toronto, Toronto, Ontario M5S 2S2, Canada

ABSTRACT A voltage-gated K⁺ conductance resembling that of the human *ether-à-go-go*-related gene product (HERG) was studied using whole-cell voltage-clamp recording, and found to be the predominant conductance at hyperpolarized potentials in a cell line (MLS-9) derived from primary cultures of rat microglia. Its behavior differed markedly from the classical inward rectifier K⁺ currents described previously in microglia, but closely resembled HERG currents in cardiac muscle and neuronal tissue. The HERG-like channels opened rapidly on hyperpolarization from 0 mV, and then decayed slowly into an absorbing closed state. The peak K⁺ conductance–voltage relation was half maximal at –59 mV with a slope factor of 18.6 mV. Availability, assessed by a hyperpolarizing test pulse from different holding potentials, was more steeply voltage dependent, and the midpoint was more positive (–14 vs. –39 mV) when determined by making the holding potential progressively more positive than more negative. The origin of this hysteresis is explored in a companion paper (Pennefather, P.S., W. Zhou, and T.E. DeCoursey. 1998. *J. Gen. Physiol.* 111:795–805). The pharmacological profile of the current differed from classical inward rectifier but closely resembled HERG. Block by Cs⁺ or Ba²⁺ occurred only at millimolar concentrations, La³⁺ blocked with K_i = ~40 μM, and the HERG-selective blocker, E-4031, blocked with K_i = 37 nM. Implications of the presence of HERG-like K⁺ channels for the ontogeny of microglia are discussed.

KEY WORDS: human *ether-à-go-go*-related gene • inward rectifier • ion channels • inactivation • *erg*

INTRODUCTION

Microglia are macrophage-like cells of the brain that are capable of serving typical phagocytic functions. However, excessive microglial activity may play a pernicious role in Alzheimer's disease, AIDS-associated dementia, and other diseases (Streit and Kincaid-Colton, 1995). There is a long-standing controversy regarding the origin of microglia (reviewed by Theele and Streit, 1993). Although it is generally accepted that they are derived from mesoderm (del Rio-Hortega, 1932; for a contrary view, see Schelper and Adrian, 1986; Fedoroff, 1995), it is not clear whether they entered the fetal brain directly from a distinct pool of myelomonocyte stem cells or first entered the bloodstream as circulating monocytes (reviewed in Ling and Wong, 1993). Microglia resemble macrophages both in the types of ion channels they express and in their plasticity; i.e., the ability to alter their pattern of ion channel expression

in response to their environment (reviewed in DeCoursey and Grinstein, 1998). Under many conditions, macrophages express inward rectifier K⁺ channels. In rat microglia in culture, we observed inward K⁺ currents, but with properties quite distinct from inward rectifier, and closely resembling those of the human *ether-à-go-go*-related gene (HERG)¹ product. To our knowledge, this is the first report of HERG channels in any immune cell, including monocytes, macrophages, and related cell lines. The presence of this novel channel type is consistent with microglial ontogeny distinct from that of bone marrow–derived circulating monocytes/macrophages.

HERG K⁺ channels have been the focus of intense interest after the discovery that HERG mutations contribute to the genetic heart disease “long QT syndrome” (Curran et al., 1995). HERG (Warmke and Ganetzky, 1994) has been identified as encoding I_{Kr}, a K⁺ channel of human cardiac myocytes (Sanguinetti et al., 1995). I_{Kr} has been characterized in cardiac myocytes (Shibasaki, 1987; Sanguinetti and Jurkiewicz, 1990a), but mRNA for *erg* is present in a number of different tissues

Portions of this work were previously published in abstract form (Zhou, W., F.S. Cayabyab, P.S. Pennefather, L.C. Schlichter and T.E. DeCoursey. 1998. *Biophys. J.* 74:A109).

Address correspondence to Tom DeCoursey, Department of Molecular Biophysics and Physiology, Rush Presbyterian St. Luke's Medical Center, 1653 West Congress Parkway, Chicago, IL 60612. Fax: 312-942-8711; E-mail: tdecours@rpslmc.edu

¹Abbreviations used in this paper: E_K, Nernst potential for K⁺; g_K, K⁺ conductance; HERG, human *ether-à-go-go*-related gene (*erg*) and its product; IR, inwardly rectifying K⁺ channel.

(Wymore et al., 1997). K^+ currents closely resembling HERG have been described in mammalian neuroblastoma cells (Arcangeli et al., 1995; Faravelli et al., 1996; Hu and Shi, 1997), quail neural crest cells (Arcangeli et al., 1997), *Xenopus* oocytes (Bauer et al., 1996), GH₃ cells (Weinsberg et al., 1997), and in the present study in rat microglia. In this paper, we characterize the electrophysiological, kinetic, and pharmacological properties of the HERG-like K^+ current in microglia. Comparison of the properties of this current with HERG reveals general similarities, but also some apparent differences. We speculate that the HERG-like K^+ channels in microglia are closely related but not identical to HERG channels. In a companion paper (Pennefather et al., 1998), we propose a simple kinetic model that describes the gating of these channels.

MATERIALS AND METHODS

Microglia Cell Culture

Microglia were isolated from brain explants of 2–3-d-old Wistar rats using a modified version of established protocols (see Schlichter et al., 1996, for detailed methods and references). In brief, neopallial tissue was digested in minimal essential medium containing 0.25% trypsin and 25 μ g/ml DNase I (all from Sigma Chemical Co., St. Louis, MO), triturated, and centrifuged to remove cell debris. The pelleted cells were resuspended in complete culture medium (MEM, 5% horse serum, 5% fetal bovine serum, 50 μ g/ml gentamicin), seeded into tissue culture flasks and fed on day 7. After 12 days, flasks were shaken (180 rpm, 15 h), floating cells were replated, allowed to adhere 1.5–2 h, and then gently shaken by hand for 5 min to remove any remaining astrocytes. At this stage, the cultures were >95% microglia, as determined by labeling all cells with nuclear dyes, acridine orange or propidium iodide (Molecular Probes, Inc., Eugene, OR), the living or fixed microglia with isolectin B4 (Streit, 1990), and the fixed and permeabilized astrocytes with an antibody directed against glial fibrillary acidic protein (both from Sigma Chemical Co.). Thereafter, the weekly feedings were supplemented with supernatant collected from the mouse fibroblast cell line, LM 10-5 (gift of Dr. S. Fedoroff, University of Saskatchewan, Saskatoon, Saskatchewan, Canada), which secretes large amounts of CSF-1, a well-known stimulus of microglia proliferation (Fedoroff et al., 1993).

After several weeks in culture, it was often possible to withdraw the CSF-1 containing supernatant and continue to grow the cells in complete culture medium for many passages. Inasmuch as the cells continued to proliferate without added growth factors, we call this a cell line. All cells in the present study were from the line that we have called MLS-9. (We have confirmed the presence and fundamental properties of the HERG-like current in two other similarly derived cell lines.) The cells stained positive with several microglia markers: 100% with isolectin B4 (Streit, 1990), 100% with DiI-acetylated LDL and Lucifer Yellow (markers for microglial endocytosis and pinocytosis; Booth and Thomas, 1991; Giulian, 1997), 98% with OX-42 antibody, and 99% with ED-1 antibody (Booth and Thomas, 1991). They did not label with antibodies against the astrocyte protein, glial fibrillary acidic protein (0%), or the fibroblast protein, fibronectin (0%), under conditions that clearly stained astrocytes and fibroblasts in primary mixed cultures. A manuscript further describing these properties of the MLS-9 cells is in preparation.

Electrophysiology

For patch-clamp recording, adherent microglia cells were released by incubating for 15 min in citrate solution (130 mM NaCl, 15 mM Na citrate, 10 mM HEPES, 10 mM d-glucose, pH 7.4), and then plated onto glass coverslips at least 2 h before recording. A coverslip bearing microglia was placed in a superfusion bath on the stage of an inverted microscope. Experiments were carried out in two separate labs using slightly different equipment and solutions. Most of the experiments on current kinetics were performed at the Rush Presbyterian St. Luke's Medical Center, while most of the pharmacological characterization was performed at the Toronto Hospital Research Institute and the University of Toronto. In Chicago, micropipettes were pulled in several stages using a Flaming Brown automatic pipette puller (Sutter Instruments Co., San Rafael, CA) from EG-6 glass obtained from Garner Glass Co. (Claremont, CA). Pipettes were coated with Sylgard 184 (Dow Corning Corp., Midland, MI) and heat-polished to a tip resistance measured in bath saline of typically 2–5 M Ω . Both pipette and the initial bath solutions were filtered with 0.22- μ m pore diameter filters (Millipore Corp., Bedford, MA). The current signal from the patch clamp (Axopatch 1A; Axon Instruments Inc., Burlingame, CA) was digitized and stored in computer files for off-line analysis using Indec Laboratory Data Acquisition and Display Systems (Indec Corp., Sunnyvale, CA) and pCLAMP 6.0.3 (Axon Instruments Inc.). In Toronto, a pipette puller (PP83; Narashige USA, Inc., Greenvale, NY) was used to fabricate electrodes from thick-walled borosilicate glass capillaries (WPI, Sarasota, FL) that were neither fire polished nor coated and typically had resistances of 5–10 M Ω , and a series resistance of 15–30 M Ω after breakthrough. An Axopatch 200A amplifier (Axon Instruments Inc.) was used to record currents and both series resistance and capacitance compensation were performed using the patch-clamp circuitry before data were digitized. Currents were acquired and analyzed using pCLAMP 6.0 software. All experiments were done at room temperature (20–23°C).

Solutions

Solutions are listed in Table I. Most salts and buffers were purchased from Sigma Chemical Co. Methanesulfonate⁻ (MeSO₃⁻) salts were prepared by titrating methanesulfonic acid (Aldrich Chemical Co., Milwaukee, WI) with the appropriate cation hydroxide to make a 1-M stock solution from which the solutions were prepared. Except where stated otherwise, liquid junction potentials were not corrected. When used, correction was based on calculated junction potentials between the bath, pipette, and ground agar bridge solutions (see Barry and Lynch, 1991). Except where noted, bath and pipette K^+ salines contained MeSO₃⁻ as the principal anion. At the Toronto Hospital Research Institute and the University of Toronto, the bath and pipette K^+ salines differed somewhat from those used at the Rush Presbyterian St. Luke's Medical Center, mainly in the use of aspartate⁻ as the intracellular anion (Table I). No differences in the properties of the HERG-like currents were noted. In the absence of internal ATP, some current rundown was seen during ~30-min recordings. For pharmacological experiments, 2 mM ATP was added to the pipette solution to prolong a stable baseline. In some cells, an outwardly rectifying, time-invariant current was observed, which resembled a swelling-sensitive anion current previously described in primary rat microglia. In both primary cells and the cell line, it was inhibited by flufenamic acid and ran down within minutes in the absence of ATP in the pipette. When calculating HERG current amplitudes for pharmacological studies, this time-invariant current was subtracted, either as the current remaining after the

TABLE 1
Composition of Saline Solutions (mM)

Name	KCl	K-anion	NaCl	CaCl ₂	MgCl ₂	EGTA	HEPES
Standard	4.5	—	160	2	1	—	5
KCl	160	—	—	2	1	—	10
KMeSO ₃	—	160	—	2	1	—	10
K aspartate	—	130	—	1	1	—	10
*KMeSO ₃	—	160	—	1	2	11	10
*K aspartate	—	130	—	2	1	10	10
*KCl	160	—	—	1	2	11	10

*Pipette solution. K-anion solutions are named according to the predominant anion (Cl⁻, MeSO₃⁻, or aspartate⁻). Solutions were titrated with the hydroxide of the predominant cation to pH 7.4 for extracellular solutions or pH 7.2 for pipette solutions. Liquid junction potentials relative to standard saline solution were 11.1 mV for KMeSO₃ and 4.5 mV for KCl. Most measurements were made with KMeSO₃ solutions.

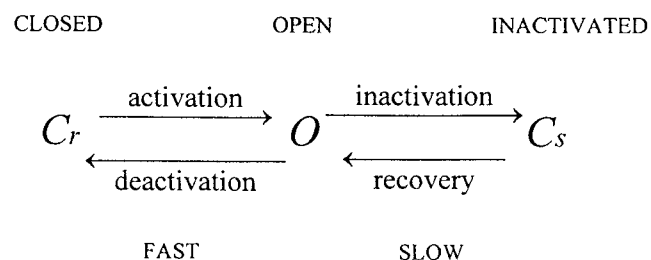
HERG channel closed at very negative potentials or after maximal block by E-4031. E-4031 is a class III antiarrhythmic methanesulfonanilide drug (Sanguinetti and Jurkiewicz, 1990a). The E-4031 used here was manufactured by Merck Research Labs (White House Station, NJ).

RESULTS

Inward K⁺ Currents

General description. Voltage-gated inward K⁺ currents were observed in nearly every microglial cell studied. The general appearance of these currents is illustrated in Figs. 1 and 2. The families of whole-cell currents in Fig. 1 were obtained in isotonic K⁺ solutions. When the holding potential (V_{hold}) was -80 mV (Fig. 1 A), 300-ms depolarizing pulses did not elicit detectable time-dependent currents. However, when hyperpolarizing pulses were applied from $V_{\text{hold}} = 0$ mV (Fig. 1 B), large inward currents were observed that increased to a peak, and then decayed more slowly. A simple interpretation is that the current is activated by hyperpolarization and subsequently inactivates. No currents are seen during pulses from $V_{\text{hold}} = -80$ mV (Fig. 1 A), because at large negative potentials all of the channels are inactivated, defined as “a refractory or inactivated condition from which [the channel] recovers at a relatively slow rate” (Hodgkin and Huxley, 1952). As is discussed in more detail in the companion paper (Pennefather et al., 1998), various terminologies have been used to describe HERG and related currents. In describing our results, we will define activation as the fast onset of current with hyperpolarization, and inactivation as the slower closing to a state C_s that follows this opening. The term deactivation will be used to describe the rapid closing to a state C_r that occurs at depolarized potentials. The following general conceptual scheme (Scheme I), in which hyperpolarization favors $C_r \rightarrow O$

and $O \rightarrow C_s$ transitions and depolarization favors the reverse, will be used to describe the data.



(SCHEME 1)

As can be seen in Fig. 1 B, both activation and inactivation became faster at more negative potentials. The inactivation rate was especially voltage sensitive, with little or no inactivation during pulses to -40 mV, and rapid and substantial inactivation at large negative potentials, resulting in cross-over of the currents. One feature apparent in Fig. 1 A is that, after 300-ms pulses to large positive potentials, large inward currents were activated upon repolarization to -120 mV in high K⁺ saline. This indicates that the proportion of channels in a resting closed state (C_r) available for activation increases at large positive potentials and that the rate and/or completeness of this return to an available state increases with depolarization. This process is equivalent to recovery from classical inactivation. The reverse nomenclature is sometimes used to describe HERG currents.

[K⁺]_o dependence of the currents. Fig. 2 compares the behavior of the HERG-like conductance during identical pulse protocols in standard (low K⁺) saline (A) and high K⁺ saline (B). In both, the holding potential was 0 mV, where most channels are in the rapidly gating closed state C_r , enabling rapid activation on hyperpolarization. In Fig. 2, the current at the beginning of pulses to large negative potentials appears to be somewhat greater than the leak current. In addition, the small outward currents in Fig. 2 B decayed as the channels deactivated at more positive potentials. Both observations suggest that some channels were already open at $V_{\text{hold}} = 0$ mV. The K⁺ currents in most cells were small in standard (low K⁺) saline, consistent with the strong dependence of the maximal conductance of HERG on external K⁺ concentration (Sanguinetti et al., 1995; Schönherr and Heinemann, 1996; Wang et al., 1997). For this reason, we explored the properties of this conductance mainly in high K⁺ saline.

K⁺ selectivity. The apparent reversal potential, V_{rev} , was -78.0 ± 7.9 mV (mean \pm SD) in standard saline solution ($[K^+]_o = 4.5$ mM) in eight cells selected for relatively small leak currents (<10 pA at -100 mV) and -1.9 ± 4.8 mV (corrected for liquid junction potentials, but without leak correction) in 12 cells in KCl saline. Thus, the channels underlying the voltage- and

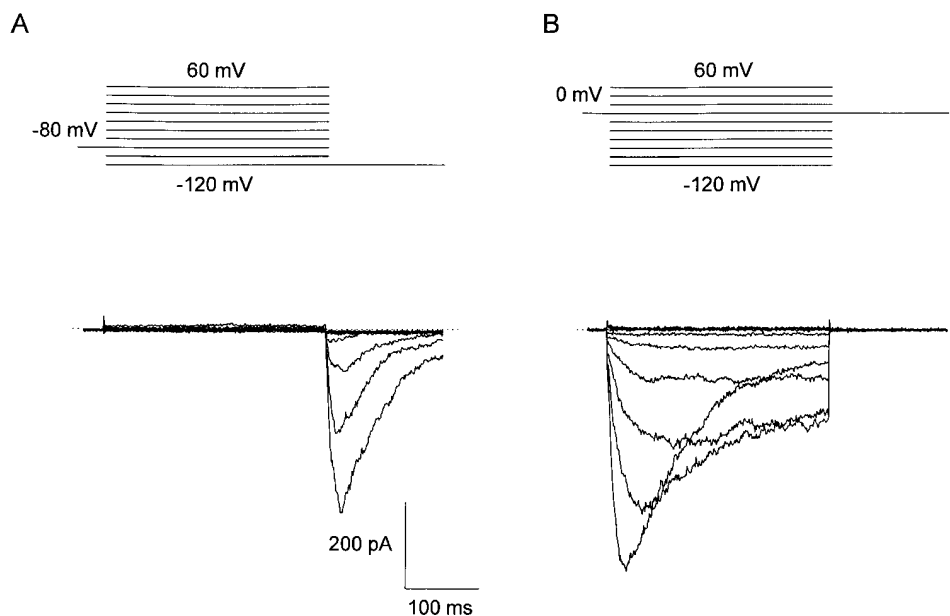


FIGURE 1. Whole-cell currents in rat microglial cells in KCl saline (pipette and bath). (A) Currents were elicited by voltage steps from -120 to 60 mV in 20 -mV increments, from $V_{\text{hold}} = -80$ mV. (B) Currents in the same cell elicited by identical voltage steps, but from $V_{\text{hold}} = 0$ mV. Voltage steps were given at 15 -s intervals, from negative to positive potentials. Calibration bars apply to both parts.

time-dependent currents activated on hyperpolarization are K^+ selective.

Gating Kinetics and Voltage Dependence

Voltage dependence of activation. Fig. 3 A shows the average normalized peak current–voltage relationship measured in K^+ saline during families of voltage-clamp pulses from $V_{\text{hold}} = 0$ mV. There is distinct inward rectification, with large inward and small outward currents. In 48 cells with a capacity of 18.4 ± 5.6 pF (mean \pm SD), the mean current at -120 mV was -565 ± 250 pA (mean \pm SD, without leak subtraction). This corresponds with an average chord conductance of 2.6 pS/ μm^2 (assuming a capacitance of 1 $\mu\text{F}/\text{cm}^2$). Because

the instantaneous current–voltage relationship was linear (see Fig. 5 B, below), the voltage dependence of channel opening can be estimated directly from the peak K^+ conductance (g_K) during voltage pulses. The average peak g_K –voltage relationship is plotted in Fig. 3 B, along with the best-fitting Boltzmann curve. The midpoint of the curve was -59 mV, and the slope factor was 18.6 mV.

Steady state availability of the K^+ conductance. The voltage dependence of availability (the converse of inactivation) of the K^+ conductance was assessed by applying test pulses to -120 mV from various holding potentials (Fig. 4, A and B). The inward test currents have characteristic rising and falling phases as channels first activate and then inactivate. At large negative V_{hold} , no

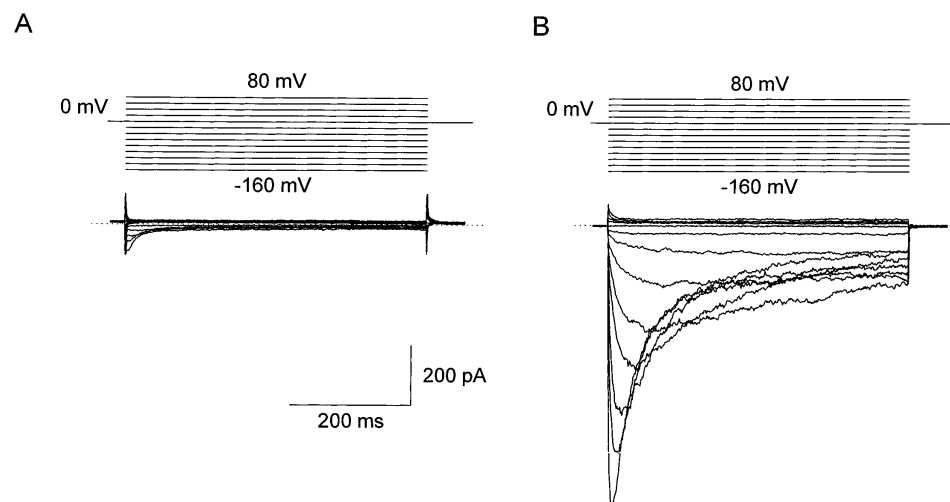


FIGURE 2. Currents recorded in standard (low K^+) saline (A) and in the same cell in KCl saline (B), with KCl in the pipette. Voltage steps in both were applied from 80 to -160 mV in -20 -mV increments every 15 s from $V_{\text{hold}} = 0$ mV. Calibration bars apply to both parts.

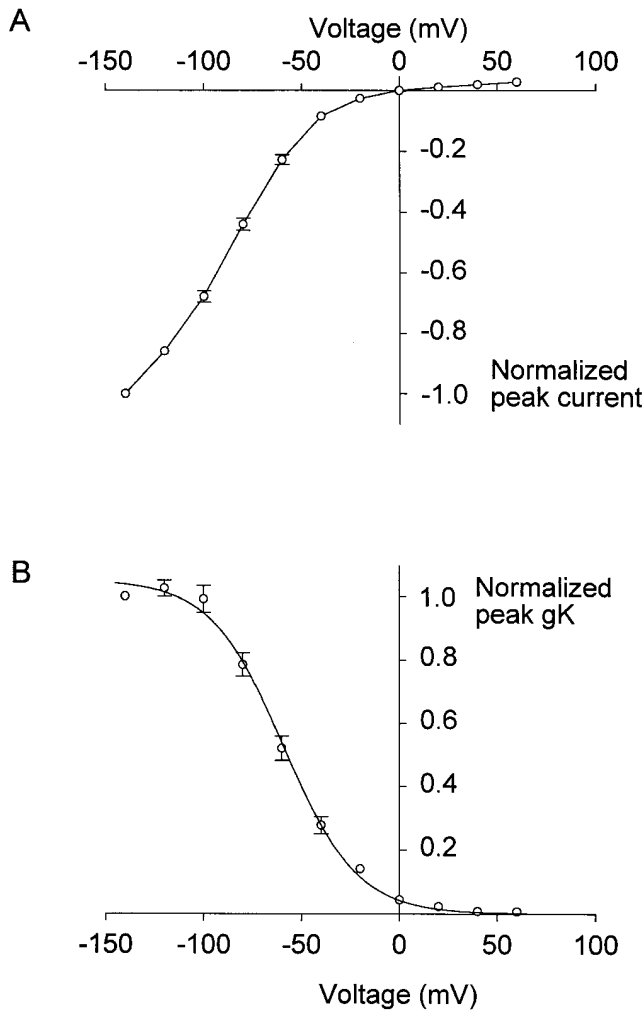


FIGURE 3. (A) Average normalized peak current–voltage relationship in KMeSO_3 saline (pipette and bath). Families of currents were obtained by applying voltage steps between -140 and 60 mV in 20 -mV increments from $V_{\text{hold}} = 0$ mV, and then repeating the same pulses in reverse order. There was little consistent hysteresis, so the currents plotted are the average from both protocols in each of five cells. Data were normalized to the current at -140 mV and are plotted without leak correction as mean \pm SEM. (B) The average chord conductance–voltage relationship in K^+ saline. The curve shows the best-fitting Boltzmann relationship:

$$\frac{g_K}{g_{K, \text{max}}} = \frac{1}{1 + \exp\left(\frac{V - V_{1/2}}{k}\right)},$$

where g_K is the peak K^+ conductance, $g_{K, \text{max}}$ is the fitted maximal g_K , $V_{1/2}$ is the midpoint of the curve, and k is a slope factor. The values obtained from averaged g_K data were -59 mV (corrected for junction potentials) for $V_{1/2}$ and 18.6 mV for k . Leak subtraction was based on the current at large positive potentials.

channels were available for activation by the step to -120 mV, and no inward test current was elicited. (In terms of our model, nearly all channels were in C_s [inactivated] states and few were in the C_r [resting] state.) When V_{hold} was positive to 0 mV, the availability was

maximal. The availability, evaluated as the normalized peak inward test current (I/I_{max}), is plotted against the prepulse potential in Fig. 4 C. This figure illustrates hysteresis in the availability measured when V_{hold} was made progressively more positive (\bullet) versus more negative (\square). V_{hold} was maintained for ~ 20 s at each potential before the test pulse was applied. Evidently, 20 s is not long enough for the system to achieve steady state, although the slowest time constants observed by direct measurements of gating kinetics were only several seconds (see Fig. 8, below). Even when V_{hold} was maintained for 60 s at each potential, hysteresis was observed. Shifts in the voltage dependence of inactivation analogous to voltage shifts in various voltage-gated channel properties seen in many cells after achieving whole-cell configuration (Fenwick et al., 1982; Fernandez et al., 1984) cannot explain this phenomenon; similar hysteresis was observed during repeated measurements in the same cell. Therefore, the hysteresis must reflect the existence of a previously unknown ultra-slow gating process (Pennefather et al., 1998).

To compare the behavior of HERG-like currents in microglia with those in other cells, we fitted the availability data with a Boltzmann function normalized to the peak test current when $V_{\text{hold}} = 40$ mV. For measurements in which V_{hold} was made progressively more positive, starting at $V_{\text{hold}} = -100$ mV (Fig. 4, \bullet), the midpoint, $V_{1/2}$, was -14 mV and the slope factor, k , was 7.7 mV. In contrast, when V_{hold} was initially 40 mV, and then progressively hyperpolarized (Fig. 4, \square), $V_{1/2}$ was -39 mV and k was 9.5 mV. Clearly, the method of making this measurement strongly influences the results. In earlier experiments, we used 2 -s prepulses (from $V_{\text{hold}} = -80$ mV), and $V_{1/2}$ averaged $+13.5$ mV in six cells. The variability in the $V_{1/2}$ values reported in the literature (see Table II) may reflect the existence of an ultra-slow gating process in other HERG-related channels.

Window currents. The overlap we observed between peak g_K vs. voltage and availability vs. voltage relationships suggests the possibility of “window currents” that might occur in intact microglia. It is evident in the records in Fig. 4 A that a window current exists after 20 s at each V_{hold} just before applying a test pulse. That this current is due to HERG-like channels (as opposed to leak or anion current) is evident from the reduction of inward current upon the return to V_{hold} after each test pulse, reflecting the inactivation of most K^+ channels during the test pulse. The voltage dependence of this window current is plotted in Fig. 4 D. Much smaller window currents were seen when V_{hold} was made progressively more positive (Fig. 4 D, \bullet). Like the availability curves in Fig. 4 C, the window current measurement thus exhibited pronounced hysteresis. The peak on the hyperpolarizing branch occurred at -40 mV and when

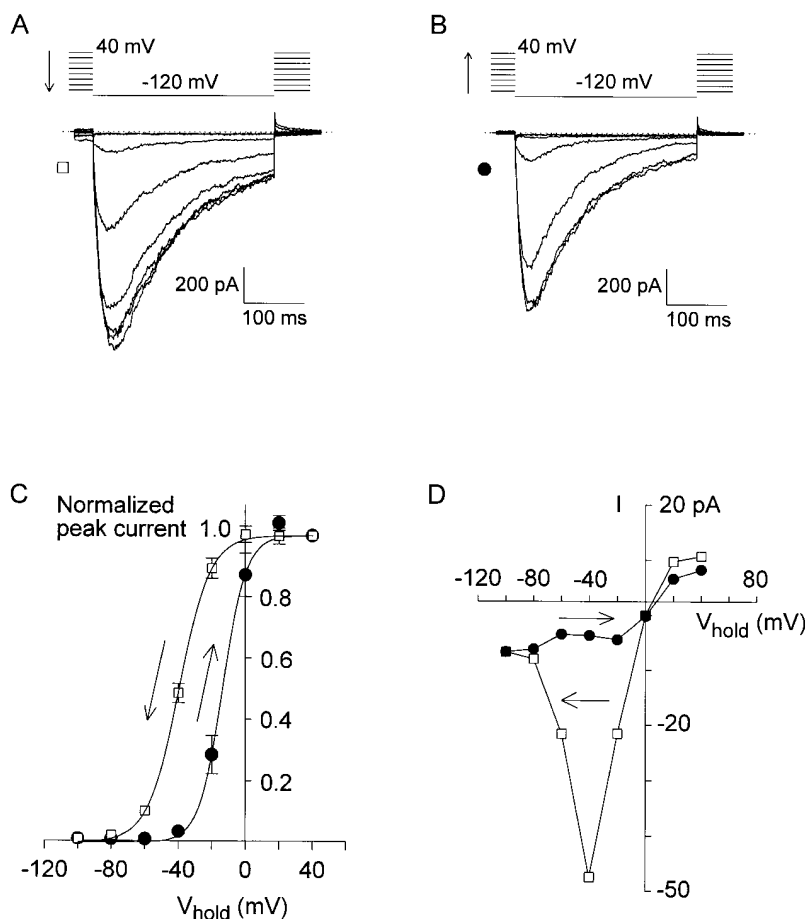


FIGURE 4. Hysteresis in the voltage dependence of quasi-steady state inactivation (inverse of availability) in KMeSO_3 (pipette and bath). (A) Superimposed are currents recorded during test pulses to -120 mV, from various V_{hold} . V_{hold} was changed progressively from 40 to -100 mV in -20 -mV increments and was maintained for ~ 20 s at each potential before the test pulse was applied. (B) Test currents from analogous measurements in the same cell as in A in which V_{hold} was increased from -100 to 40 mV. (C) Average peak test current amplitudes ($n = 4$ cells) are plotted as a function of V_{hold} , normalized to the test current from $V_{\text{hold}} = 40$ mV. In a few cells in which V_{hold} was changed up to 80 mV, there was no further enhancement of the test current beyond that at $V_{\text{hold}} = 40$ mV. In each cell, measurements were made both by changing V_{hold} from -100 to 40 mV (\bullet) and from 40 to -100 mV (\square), not always in the same order. The “up” and “down” relationships (arrows) were fitted to a Boltzmann function:

$$\frac{I}{I_{\text{max}}} = \frac{1}{1 + \exp\left(\frac{V_{1/2} - V}{k}\right)},$$

where I_{max} is the peak test current when $V_{\text{hold}} = 40$ mV. For measurements in which V_{hold} was made progressively more positive, starting at $V_{\text{hold}} = -100$ mV (B, \bullet), the midpoint, $V_{1/2}$, was -14 mV and the slope factor, k , was 7.7 mV. When V_{hold} was initially 40 mV, and then progressively hyperpolarized (A, \square), $V_{1/2}$ was -39 mV and k was 9.5 mV. (D) Window currents from the experiment illustrated in A and B. The current at V_{hold} was measured just before each test pulse, and is plotted vs. V_{hold} . Distinct window currents were seen consistently in other cells when the protocol in A was used, whereas the window currents measured using the protocol in B were very small.

converted to conductance was 14% of $g_{\text{K,max}}$ in that cell. In four cells analyzed in this way, the window current at -40 mV averaged $13.6 \pm 0.5\%$ of $g_{\text{K,max}}$ (mean \pm SD). The model described in the next paper (Pennefather et al., 1998), using rate constants consistent with experimental observations, predicts a peak window conductance (at -36 mV) of $\sim 12\%$ of the maximal conductance.

The instantaneous current–voltage relation. The instantaneous current–voltage relationship was determined from experiments like the one in Fig. 5 A. The K^+ conductance was activated by a brief pulse to -120 mV from $V_{\text{hold}} = 0$ mV, and then the voltage was stepped to a range of potentials. The test current at most potentials decayed rapidly as channels closed. The amplitude of the “instantaneous” current was obtained by fitting the decay with a single exponential and extrapolating to the start of the test pulse. When measured in K^+ saline, the resulting instantaneous current–voltage relation was essentially linear between -80 and 80 mV (Fig. 5 B). Thus, the strong inward rectification of the mac-

rosopic current is due mainly to voltage-dependent gating and not to intrinsic rectification of the open channel current.

Activation and deactivation kinetics. When fitted by single exponentials, the time constants of channel opening and closing were moderately voltage dependent, as illustrated in Fig. 6. The activation time constant, τ_{act} (Fig. 6, \square), measured during the turn-on of currents during hyperpolarizing pulses (e.g., Figs. 1 and 2) was ~ 30 ms at -60 mV, decreasing e -fold in 54 mV to < 10 ms at -120 mV.

Deactivation was evaluated in “tail current” experiments like the one illustrated in Fig. 5 A. The test current at most potentials decayed rapidly as channels closed, in terms of our model, predominantly into state C_r . The time constant of current decay, τ_{tail} (Fig. 5 A, \bullet), was faster at more positive potentials, decreasing with depolarization e -fold in 104 mV. τ_{tail} passed through a local maximum at -40 mV of ~ 35 ms. It is noteworthy that τ_{act} and τ_{tail} were identical at -60 mV, consistent with a simple first-order transition between a single

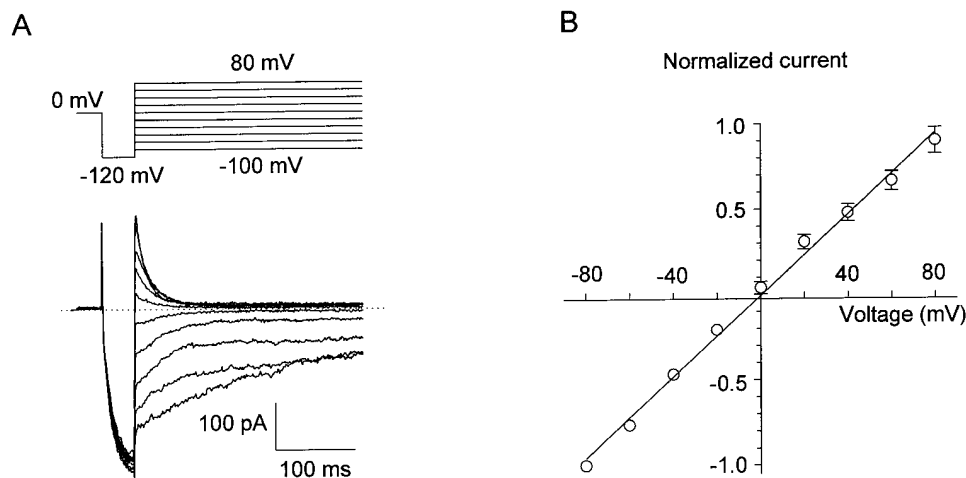


FIGURE 5. Tail current and instantaneous current-voltage relationship measurements in KMeSO_3 (pipette and bath). (A) Tail currents were recorded with voltage steps from -100 to 80 mV in 20 -mV increments at 15 -s intervals, after a 30 -ms prepulse to -120 mV, from $V_{\text{hold}} = 0$ mV. (B) The average instantaneous current-voltage relation (\pm SEM), normalized to the initial current at -80 mV ($n = 7$). The currents during test pulses were fitted with a single exponential, and extrapolated to the beginning of the voltage step.

open and a single closed state. At potentials more negative than -60 mV, the time constant of current decay measured with the tail current protocol of Fig. 5 A increased progressively, and with an increased variability. Channels in this negative voltage range appear to enter another closed state (C_s) that behaves like an inactivated state. It can be seen in Fig. 5 A that beginning at -20 mV and increasingly at more negative potentials,

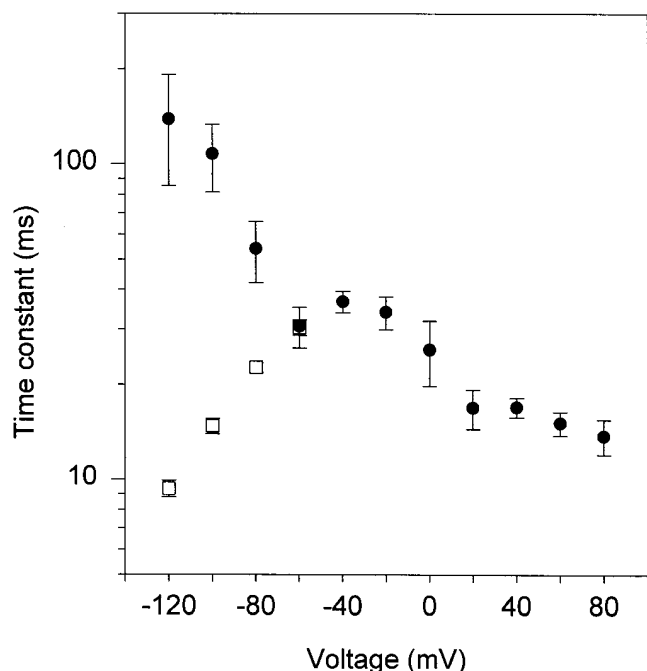


FIGURE 6. Time constants of activation (τ_{act} , \square) and deactivation (τ_{tail} , \bullet) in KMeSO_3 (pipette and bath). The rising phase of currents during hyperpolarizing pulses from $V_{\text{hold}} = 0$ mV was fitted with a single exponential to obtain τ_{act} . Tail currents like those in Fig. 5 A were fitted with a single exponential to obtain τ_{tail} . Plotted values are the mean \pm SEM of $n = 22$ and 7 cells for τ_{act} and τ_{tail} , respectively.

the rapid closing process (to C_r) becomes less complete. This result is consistent with the voltage dependence of the rapid $C_r \leftrightarrow O$ transition shown in Fig. 3 B, and with the existence of a window current (Fig. 4 D). At larger negative potentials, the current again decayed, but anomalously slowly, most likely due to channels inactivating (entering slowly equilibrating closed C_s states), rather than deactivating into the resting C_r state. The observed current decay at potentials more negative than -60 mV is thus a mixture of two types of closing, with the slow $O \rightarrow C_s$ pathway becoming dominant at more negative potentials. Indeed, at -120 mV, the time constant measured with this protocol is identical to that of inactivation measured with the inactivation protocol (see Fig. 8). Further evidence supporting this interpretation is presented in the following paper (Pennefather et al., 1998).

The kinetics of inactivation (slow closing). The time constants of inactivation (τ_i) and recovery (τ_{recovery}) were more strongly voltage dependent than those of activation (τ_{act}) and fast closing (τ_{tail}). Recovery from inactivation at moderate potentials was slow. Recovery was evaluated in paired-pulse experiments like the one illustrated in Fig. 7. From $V_{\text{hold}} = 0$ mV, most of the channels opened, and then were inactivated during a pulse to -120 mV. The potential was returned to 0 mV and after a variable interval a second pulse to -120 mV was applied. The amplitude of the inward current during the second pulse reflects the recovery from inactivation that took place at 0 mV in the interval between pulses. It is apparent that recovery required several seconds and was not yet complete after the largest interval illustrated (4 s). In other experiments, recovery was measured at different potentials. The peak current during the second pulse as a function of the interval between pulses was fitted by a single exponential to obtain τ_{recovery} . At -20 to -40 mV, recovery seemed to be slow and incomplete, and reliable data were not ob-

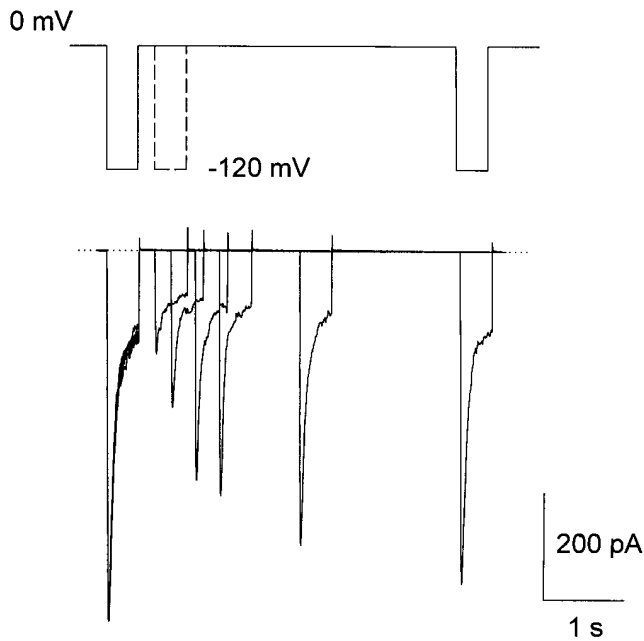


FIGURE 7. Recovery from the inactivation at 0 mV in KMeSO_3 (pipette and bath). Superimposed are currents recorded during pairs of identical 300-ms pulses to -120 mV applied from $V_{\text{hold}} = 0$ mV, separated by an interval of variable duration. The whole pulse protocol was given once every 30 s. To explore recovery at other voltages, the potential in the interval between pulses was varied. The time constant of recovery, τ_{recovery} , was obtained by fitting the envelope of peak test currents to a single exponential. In this experiment, τ_{recovery} was 0.74 s.

tained. As shown in Fig. 8 (○), τ_{recovery} was strongly voltage dependent, decreasing on average e -fold in 35 mV. Recovery from inactivation could be measured directly in Cs^+ saline as a rising outward current (Pennefather et al., 1998), which showed that τ_{recovery} decreased steeply with depolarization also in Cs^+ saline.

Plotted in Fig. 8 is τ_i (●), calculated from the decay of current during hyperpolarizing pulses in K^+ saline. Inactivation first became detectable at potentials negative to -40 mV, was incomplete and quite slow at moderately negative potentials ($\tau_i \approx 10$ s at -50 mV), and then τ_i decreased at larger negative potentials e -fold in 18.3 mV (between -80 and -120 mV). At potentials negative enough for inactivation to develop rapidly, there was often a small slower component of current decay. Fast and slow components of current decay have been described previously for HERG-like currents in cardiac myocytes (Yang et al., 1994), and in HERG current expressed in *Xenopus* oocytes (Spector et al., 1996a, 1996b) or in HEK cells (Snyders and Chaudhary, 1996). We did not investigate this slow component systematically.

The time constants of both activation and inactivation appeared to be smaller in low than in high K^+ saline, but activation in low K^+ saline was not resolved

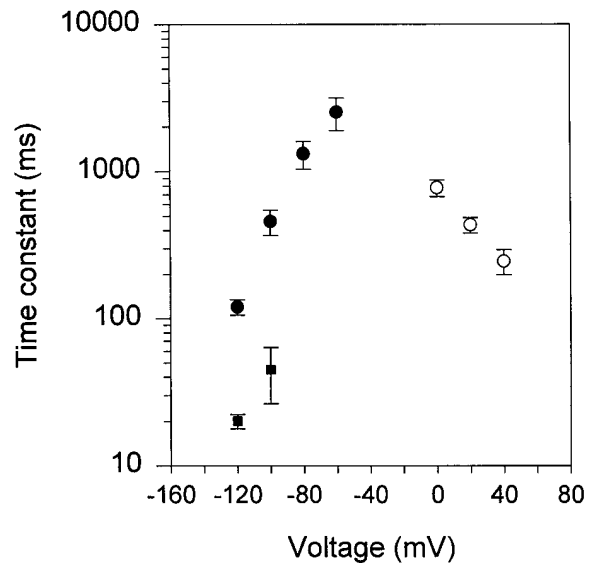


FIGURE 8. Mean time constants of inactivation, τ_i (●), and recovery, τ_{recovery} (○), measured in KMeSO_3 (pipette and bath). Decaying currents during hyperpolarizing pulses from $V_{\text{hold}} = 0$ mV were fitted with a single exponential to obtain τ_i ($n = 7$), and each envelope of peak currents during paired-pulse recordings like those illustrated in Fig. 7 was fitted with a single exponential to obtain τ_{recovery} ($n = 6$). Measurements of τ_i in standard saline are also plotted for 16 cells (■). The values of τ_i in standard and K^+ saline differ significantly at both voltages ($P < 10^{-5}$). In ~ 10 – 20% of the cells studied, inactivation appeared to be qualitatively slower than usual, although in other respects the conductance resembled HERG rather than IR. The reason for this behavior was not determined and those cells were excluded from analysis.

well enough to draw firm conclusions. In the voltage range negative to the Nernst potential for K^+ (E_{K}), τ_i was 5– $10\times$ faster in standard saline (Fig. 8, ■) than in K^+ saline. Previous studies also report that the fast gating process is accelerated by low $[\text{K}^+]_o$ (Wang et al., 1996, 1997; Yang et al., 1997), but in some studies the slower process of inactivation/recovery was not affected by $[\text{K}^+]_o$ (Shibasaki, 1987; Wang et al., 1997). In any case, it is evident that the gating kinetics are affected much less by changes in $[\text{K}^+]_o$ than are genuine inward rectifier (IR) K^+ channels.

Pharmacological Sensitivity

Compared with IR, the HERG-like K^+ currents in microglia were less sensitive to block by extracellular cations (Na^+ , Cs^+ , and Ba^{2+}), and block was only weakly time- and voltage dependent. There was no obvious time- or voltage-dependent block by Na^+ , and nearly complete inactivation of inward K^+ currents occurred both in standard saline with 160 mM Na^+ and in Na^+ -free K^+ saline (Fig. 2, A and B). This is clearly distinct from the effects of Na^+ on IR channels. As seen in Fig. 9 A, when 10 mM Ba^{2+} was added to the bath the inward current was attenuated by $>80\%$ ($n = 5$), but the

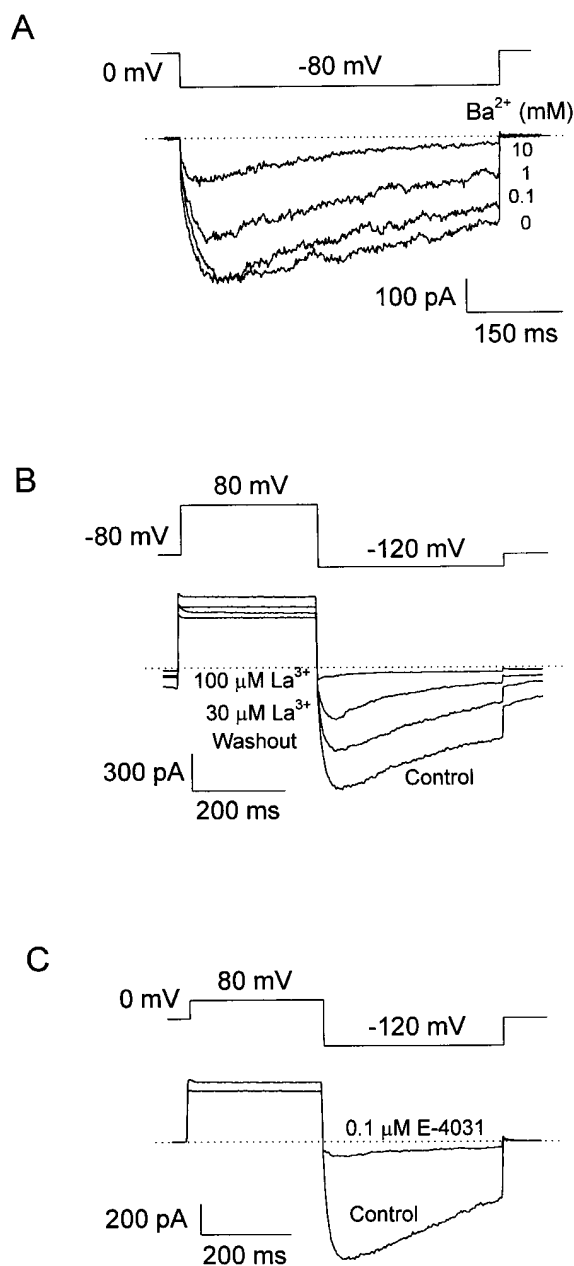


FIGURE 9. Pharmacological sensitivity of HERG-like currents. (A) Block by Ba^{2+} . Identical pulses to -80 mV from $V_{\text{hold}} = 0$ mV were applied to a cell exposed to KCl saline (pipette and bath) with the indicated concentration of BaCl_2 . (B) Block by La^{3+} in KCl saline with K aspartate in the pipette. From $V_{\text{hold}} = -80$ mV, a 300-ms prepulse to 80 mV to remove inactivation was followed by a test pulse to -120 mV. In this cell, $30 \mu\text{M}$ La^{3+} had a substantial effect and $100 \mu\text{M}$ virtually abolished the current, with partial recovery upon washout. (C) Block by 100 nM E-4031 in KCl saline with K aspartate in the pipette. Pulses to -120 mV were applied after a prepulse to 80 mV from $V_{\text{hold}} = 0$ mV. To explore a range of concentrations, control currents were recorded for at least 5 min, the lowest concentration of E-4031 was added to the bath and sufficient time was allowed for steady state blockade (usually 5 min) before the next concentration was added. The time-independent outward currents at 80 mV in B and C are most likely anion currents.

decay time constant was only slightly faster than in the control solution, in contrast to the more potent and rapid time-dependent block of IR currents in microglia (Schlichter et al., 1996) and other cells. We cannot rule out the possibility that some part of the effect of Ba^{2+} reflects the presence of a few IR channels in these cells. La^{3+} , which reportedly blocks HERG-like currents in a voltage-dependent manner (Faravelli et al., 1996), inhibited the microglial current (Fig. 9 B). There was little block at $3 \mu\text{M}$, $37 \pm 7\%$ inhibition at $30 \mu\text{M}$ (mean \pm SEM, $n = 5$), and $77 \pm 5\%$ inhibition at $100 \mu\text{M}$ ($n = 8$). The methanesulfonanilide drug, E-4031, is a classic blocker of HERG channels. HERG-like currents in microglia were sensitive to this drug, with substantial block at 100 nM (Fig. 9 C). The $K_{1/2}$ measured using the illustrated protocol was estimated to be 37 ± 8 nM ($n = 5$).

DISCUSSION

The Predominant K^+ Current in Cultured Rat Microglia Was HERG-like and not Inward Rectifier

The presence of IR K^+ currents in microglia from mouse and rat has been demonstrated repeatedly (Kettenmann et al., 1990; Banati et al., 1991; Nörenberg et al., 1992; Brockhaus et al., 1993; Eder et al., 1995a; Ilschner et al., 1995; Visentin et al., 1995; Fischer et al., 1995; Schlichter et al., 1996), although these studies also show that K^+ channel expression changes dramatically after treatment with various cytokines. IR channels in microglia exhibit classical properties of Kir2 channels, including high K^+ selectivity, $[\text{K}^+]_o$ -dependent gating, voltage-dependent block by Cs^+ , and voltage- and time-dependent block by Na^+ and Ba^{2+} (Visentin et al., 1995; Eder et al., 1995b; Schlichter et al., 1996). At a superficial level, the MLS-9 microglia preparation studied here appeared to have similar K^+ currents. However, closer inspection revealed several properties that clearly distinguish these currents from traditional IR currents.

The inward K^+ currents described here were affected only by relatively high (millimolar) concentrations of Ba^{2+} or Cs^+ . The time dependence of Ba^{2+} block was distinctly weaker than for IR channels in microglia (Schlichter et al., 1996) and other cells. Cs^+ was detectably permeant so that in isotonic Cs^+ solution, distinct inward and larger outward currents were observed (Pennefather et al., 1998), as reported previously for HERG (Schönherr and Heinemann, 1996).

Macroscopic IR currents in many cells exhibit voltage- and time-dependent block by extracellular Na^+ and slower, weak block by Ca^{2+} and Mg^{2+} (Biermans et al., 1987), but little genuine inactivation. The decay of IR currents in primary cultures of murine microglia also appears to be due to Na^+ block (Eder et al., 1995a). In contrast, the HERG-like currents described

here exhibited a strongly voltage-dependent inactivation (slow closing) process. Although τ_i was faster in standard (high Na^+) saline than in Na^+ -free K^+ saline (Fig. 8), the current decayed almost completely at large negative potentials in the complete absence of Na^+ . Thus, the decay cannot be attributed to block by Na^+ .

A defining property of IR currents is their dependence on $[\text{K}^+]_o$. In a variety of cells, opening of IR channels shows a nearly perfect dependence on $[\text{K}^+]_o$, such that the kinetics of opening and the conductance-voltage relation nearly superimpose when plotted as a function of $V-E_K$ (Almers, 1971; Hestrin, 1981; Harvey and Ten Eick, 1988; Silver and DeCoursey, 1990; Pennefather et al., 1992). Consistent with other studies (Wang et al., 1997; Yang et al., 1997), activation of the HERG-like current in microglia appeared to be somewhat faster in low than high $[\text{K}^+]_o$. In contrast, lowering $[\text{K}^+]_o$ slows the activation of IR channels at a given voltage. Also in stark contrast to IR channels, we found little effect of $[\text{K}^+]_o$ on the position of the g_K - V relationship, consistent with previous studies of HERG-like currents in neuroblastoma (Arcangeli et al., 1995), and HERG in which $V_{1/2}$ shifted only 30 mV when E_K was changed by 99 mV (Wang et al., 1997).

Are HERG-like K^+ channels expressed in microglia in situ? There are numerous reports of IR channels in microglia in primary culture. We did not observe IR currents in the MLS-9 cell line derived from microglia, and instead consistently observed HERG-like K^+ currents. Clearly, the pattern of K^+ channel expression is different in MLS-9 cells and in microglia in primary culture. This is not too surprising in light of the well-established propensity of cultured microglia to change their pattern of ion channel expression. The properties of the K^+ currents reported previously in microglia identify them unambiguously as IR. An important question is whether HERG-like K^+ channels are expressed in microglia in situ under any circumstances. In preliminary experiments (Cayabyab, F.S., and L.C. Schlichter, unpublished observations), we have explored the possible expression of HERG-like K^+ current in cultured microglia soon after isolation, using E-4031 to distinguish it from classical IR. Large currents with properties very similar to those described herein were seen in a small number of microglia, under apparently specific conditions that have not yet been fully worked out. It may well be that this current was not discovered earlier in microglia because in most studies the conditions used would minimize the HERG-like current: low extracellular K^+ (Fig. 2 A), and a negative V_{hold} that would inactivate HERG-like channels almost entirely (Fig. 1 A).

Implications for the ontogeny and functions of microglia. There is a long-standing debate over whether microglia originated in the brain from embryonic precursor cells, or whether they are derived from circulating macro-

phages that migrated to the brain. A lack of delayed-rectifier K^+ current in microglia, both in culture (Kettenmann et al., 1990) and in brain slices (Brockhaus et al., 1993), initially appeared to distinguish unstimulated microglia from macrophages. However, subsequent studies have shown that microglia can express a delayed-rectifier current that is apparently identical to that in macrophages. Both cell types have Kv1.3 mRNA transcripts, suggesting that this channel underlies the observed currents (Nörenberg et al., 1993; DeCoursey et al., 1996). Delayed rectifier currents appear spontaneously in a fraction of cells (Korotzer and Cotman, 1992; Schlichter et al., 1996), and more consistently after exposure to astrocytes (Korotzer and Cotman, 1992; Sievers et al., 1994), to astrocyte-conditioned medium (Eder et al., 1997), or to Teflon™ (Nörenberg et al., 1993), and after stimulation with PMA (Yoo et al., 1996), PMA and γ -interferon (Visentin et al., 1995), lipopolysaccharide (Nörenberg et al., 1994; Illes et al., 1996), or granulocyte-macrophage colony stimulating factor (Eder et al., 1995b). Conversely, there are many situations in which macrophages do not express delayed rectifier (Ypey and Clapham, 1984; Gallin and Sheehy, 1985; Gallin and McKinney, 1988; Nelson et al., 1990; DeCoursey et al., 1996) and in which they express inward-rectifier channels (Gallin and Sheehy, 1985; Randriamampita and Trautmann, 1987; Gallin and McKinney, 1988; McKinney and Gallin, 1988, 1990; DeCoursey et al., 1996) like those described in microglia.

We demonstrate here that rat microglia cells maintained in prolonged tissue culture express HERG-like K^+ channels that, to our knowledge, have never been described in any immune cell (for review see DeCoursey and Grinstein, 1998). HERG channels were originally cloned from a brain (hippocampal) expression library (Warmke and Ganetzky, 1994), and HERG-like channels are present in neuroblastoma cells (Arcangeli et al., 1995; Faravelli et al., 1996; Hu and Shi, 1997). Their expression in microglia is thus compatible with a possible ectodermal origin (compare Schelper and Adrian, 1986; Fedoroff, 1995). If microglia originated from mesoderm, their precursor cells may have diverged from monocyte/macrophage precursor cells at a relatively early developmental stage. Alternatively, the expression of HERG-like channels in microglia may be the result of their development in the brain microenvironment.

Possible roles for HERG in microglia. Based on their near ubiquity in microglia, IR channels are widely believed to contribute most of the K^+ conductance at the resting membrane potential (Banati et al., 1991; Kettenmann et al., 1990; Korotzer and Cotman, 1992; Nörenberg et al., 1992, 1994; Fischer et al., 1995; Schlichter et al., 1996). The two stable membrane potentials that have been re-

ported for microglia (-70 and -35 mV; Nörenberg et al., 1994) are near the K^+ and Cl^- equilibrium potentials (-85 and ~ -30 mV). In cardiac muscle, HERG currents contribute to repolarization during the long action potential. There is no evidence that microglia are excitable cells. However, at least under certain conditions, microglia possess a variety of channels that upon activation would depolarize the membrane; e.g., purinergic receptor-gated (Kettenmann et al., 1993; Illes et al., 1996), Ca^{2+} (Colton et al., 1994), Na^+ (Korotzer and Cotman, 1992), and anion (Schlichter et al., 1996) channels. The MLS-9 microglial cell line studied here displayed little if any IR current and no delayed rectifier K^+ current. Inasmuch as the HERG-like current may be the only significant K^+ current in this cell line, and conceivably also in specific functional states of microglial cells, it is significant that its voltage dependence of activation and inactivation predicts a standing window current at membrane potentials within the physiological range (-50 to $+20$ mV). The substantial window currents exhibited by HERG-like channels in microglia would oppose depolarizing stimuli, such as produced by purinergic stimulation.

Quail neural crest cells during early development sequentially express HERG-like K^+ , and then classical IR K^+ , channels (Arcangeli et al., 1997). These K^+ channels appear to set the resting membrane potential in these cells, and the appearance of IR coincides with a 20-mV hyperpolarization of the membrane potential. Evidently, the voltage dependence of HERG gating results in a less negative set point for the membrane potential than E_K , whereas IR channels keep the membrane potential near E_K . It has been speculated that this more positive resting potential would reduce the excitability of immature cells and promote proliferation (Arcangeli et al., 1997).

Properties of HERG-like Currents in Microglia Compared with Other Cells

Pharmacological sensitivity. La^{3+} blocks native HERG currents in cardiac muscle, I_{Kr} , (at 10–100 μM ; Sanguinetti and Jurkiewicz, 1990b), HERG-like currents in neuroblastoma cells (at 30 μM ; Faravelli et al., 1996), and HERG expressed in *Xenopus* oocytes (>90% inhibition at 10 μM ; Sanguinetti et al., 1995). At least part of this inhibition has been attributed to a shift in surface potential and, therefore, in the apparent voltage dependence of the current (Sanguinetti and Jurkiewicz, 1990b; Sanguinetti et al., 1995). The HERG-like current in rat microglia was inhibited by La^{3+} with a K_i of ~ 40 μM . When expressed heterologously, the HERG channel (Trudeau et al., 1995; Snyders and Chaudhary, 1996), like cardiac I_{Kr} current (Sanguinetti and Jurkiewicz, 1990a), is inhibited by the methanesulfonanil-

ide drugs, E-4031 and dofetilide. K_i values reported for E-4031 range from 10 nM in GH3 cells (Weinsberg et al., 1997) and ferret atrial myocytes (Liu et al., 1996) to 397 nM in guinea pig ventricular myocytes (Sanguinetti and Jurkiewicz, 1990a) and 588 nM for HERG expressed heterologously in *Xenopus* oocytes (Trudeau et al., 1995). Block by methanesulfonanilides exhibits state dependence, interpreted as open-channel block (Carmeliet, 1992; Snyders and Chaudhary, 1996; Spector et al., 1996b), which most likely explains differences in reported potency. In microglia, E-4031 blocked with $K_i = 37$ nM, well within the range reported for HERG.

Inactivation is more steeply voltage dependent than activation. The τ_1-V , $\tau_{recovery}-V$, and steady state availability relationships of the HERG-like currents described here all were steeply voltage dependent. A similarly steep voltage dependence has been reported in all preparations in which HERG and related currents have been studied (Table II). However, the midpoint ($V_{1/2}$) is rather variable. The persistent hysteresis that we observed when measuring quasi-steady state availability curves (Fig. 4 C) shows that quite different results can be obtained if the measurement is made with different voltage protocols. Depending on the history of the measurement, $V_{1/2}$ was -39 or -14 mV when measured in the same cells using 20-s prepulses. With 2-s prepulses, $V_{1/2}$ averaged 13.5 mV. Thus, the coupling of the two closing pathways through the open state and/or the existence of additional slowly equilibrating states can dramatically influence this parameter, with $V_{1/2}$ varying by 55 mV, depending on how it is measured.

The activation process, characterized by $\tau_{act}-V$, $\tau_{tail}-V$, and peak g_K-V relationships, exhibited moderate voltage dependence, comparable with that observed in other preparations (Table II), both for HERG expressed heterologously and for endogenous HERG-like currents. The overlap of activation and inactivation appears to be smaller in microglia than in other cells, which would tend to limit the size of window current and contribute to the absence of depolarization-activated outward currents.

Gating kinetics compared. Both fast and slow gating processes in microglia appear to be similar kinetically to their counterparts in neuroblastoma cells (Arcangeli et al., 1995). Both gating processes are slower than those measured in low K^+ solutions for HERG expressed in *Xenopus* oocytes (Trudeau et al., 1995; Schönherr and Heinemann, 1996; Spector et al., 1996a; Wang et al., 1996) or in HEK cells (Snyders and Chaudhary, 1996). However, the possible $[K^+]_o$ dependence of gating complicates this comparison. The component of cardiac myocyte current believed to reflect native HERG channels (I_{Kr}) appears to inactivate and recover at least an order of magnitude faster in studies at body temperature, 35–37°C (Shibasaki, 1987; San-

TABLE II
Voltage Dependence of Activation and Inactivation of HERG and Similar Channels

Channel, preparation	Activation		Inactivation		[K ⁺] _o	Reference
	V _{1/2}	k	V _{1/2}	k		
	mV	mV	mV	mV	mM	
I _K , cardiac myocyte			-25.1	7.4	5.4-150	Shibasaki, 1987
I _{Kr} , cardiac myocyte			-21.5	7.5	4	Sanguinetti and Jurkiewicz, 1990a
I _{Kr} , cardiac myocyte	-30	22.7	-13	8.4	5.4	Liu et al., 1996
HERG, <i>Xenopus</i>			6	11.7	100	Trudeau et al., 1995
HERG, <i>Xenopus</i>	-49	28	-15	7.9	10, 2	Sanguinetti et al., 1995
HERG, <i>Xenopus</i>	-52	27	-39	8.8	4	Spector et al., 1996b
HERG, <i>Xenopus</i>	-25	26	-23.7	6.67	98	Wang et al., 1997
HERG, HEK293			-14	6.4	4	Snyders and Chaudhary, 1996
HERG, HEK293	-90	25			10	Smith et al., 1996
L, neuroblastoma	-49	18	-25.4	7.5	40	Arcangeli et al., 1995
L, F-11 neuroblastoma	-57.4	24	-52	4.8	40	Faravelli et al., 1996
L, <i>Xenopus</i>			-50		118	Bauer et al., 1996
N, NG108-15			-25		100	Hu and Shi, 1997
L, rat microglia	-59	18.6	-14, -39	7.7, 9.5	160	Present study

L, HERG-like; N, not identified as HERG-like by the authors of the study. Activation and inactivation parameters are midpoints, V_{1/2}, and slope factors, k, for simple Boltzmann fits (Figs. 3 and 4) and are defined according to the convention used here (as the faster and slower components of gating, respectively). The nomenclature varies in the original references.

guinetti and Jurkiewicz, 1990a). The closest comparison is with HERG in *Xenopus* oocytes at 21–23°C with [K⁺]_o = 98 mM (Wang et al., 1997), where τ_{act}, τ_{tail}, and τ_i appear similar to values reported here, but τ_{recovery} appears two to three times faster. Considering the differences in recording conditions, the currents described here are kinetically similar to HERG and HERG-like currents in other cells. The main difference seems to be that HERG-like currents in microglia exhibit very slow gating around -40 mV, which can lead to use-dependent phenomena.

When expressed heterologously in *Xenopus* oocytes, HERG currents have a distinct outward component in standard saline, although the outward currents are at least an order of magnitude smaller than inward cur-

rents (Spector et al., 1996a). We could detect only very small outward currents under comparable conditions in microglia. This result is predicted by our model (Pennefather et al., 1998) and arises because recovery from inactivation at positive potentials is slow, relative to the closing rate. An additional (related) factor is that activation is shifted to more negative potentials than in HERG in oocytes (Wang et al., 1997).

In summary, the biophysical and pharmacological evidence leads to the conclusion that the predominant K⁺ channel present in the rat microglial cell line studied here was not IR, but was a product of *erg* or a closely related channel gene. Which isoform is present in microglia remains to be determined.

The authors thank Claudia Eder for critically reading the manuscript, E. Wanke for generously providing a preprint, and P. Backx (Toronto Hospital Research Institute) for the E-4031.

This work was supported in part by Research Grant HL-52671 (T.E. DeCoursey) and Training Grant T32-HL07692 (W. Zhou), both from the National Institutes of Health, a Grant-in-Aid (NA-3182) from the Heart and Stroke Foundation of Ontario (L.C. Schlichter and P.S. Pennefather), and a grant from the Medical Research Council of Canada (L.C. Schlichter).

Original version received 5 August 1997 and accepted version received 18 March 1998.

REFERENCES

- Almers, W. 1971. The Potassium Permeability of Frog Muscle Membrane. Ph.D. dissertation. University of Rochester, Rochester, NY.
- Arcangeli, A., L. Bianchi, A. Becchetti, L. Faravelli, M. Coronello, E. Mini, M. Olivotto, and E. Wanke. 1995. A novel inward-rectifying K⁺ current with a cell-cycle dependence governs the resting potential of mammalian neuroblastoma cells. *J. Physiol. (Camb.)* 489:455–471.
- Arcangeli, A., B. Rosati, A. Cherubini, O. Crociani, L. Fontana, C. Ziller, E. Wanke, and M. Olivotto. 1997. HERG- and IRK-like inward rectifier currents are sequentially expressed during neuronal development of neural crest cells and their derivatives. *Eur. J. Neurosci.* 9:2596–2604.
- Banati, R.B., D. Hoppe, K. Gottmann, G.W. Kreutzberg, and H. Kettenmann. 1991. A subpopulation of bone marrow-derived macrophage-like cells shares a unique ion channel pattern with

- microglia. *J. Neurosci. Res.* 30:593–600.
- Barry, P.H., and J.W. Lynch. 1991. Liquid junction potentials and small cell effects in patch-clamp analysis. *J. Membr. Biol.* 121:101–117.
- Bauer, C.K., T. Falk, and J.R. Schwarz. 1996. An endogenous inactivating inward-rectifying potassium current in oocytes of *Xenopus laevis*. *Pflügers Arch.* 432:812–820.
- Biermans, G., J. Vereecke, and E. Carmeliet. 1987. The mechanism of the inactivation of the inward-rectifying K current during hyperpolarizing steps in guinea-pig ventricular myocytes. *Pflügers Arch.* 410:604–613.
- Booth, P.L., and W.E. Thomas. 1991. Evidence for motility and pinocytosis in ramified microglia in tissue culture. *Brain Res.* 548:163–171.
- Brockhaus, J., S. Ilschner, R.B. Banati, and H. Kettenmann. 1993. Membrane properties of amoeboid microglial cells in the corpus callosum slice from early postnatal mice. *J. Neurosci.* 13:4412–4421.
- Carmeliet, E. 1992. Voltage- and time-dependent block of the delayed K⁺ current in cardiac myocytes by dofetilide. *J. Pharmacol. Exp. Ther.* 262:809–817.
- Colton, C.A., M. Jia, M.X. Li, and D.L. Gilbert. 1994. K⁺ modulation of microglial superoxide production: involvement of voltage-gated Ca²⁺ channels. *Am. J. Physiol.* 266:C1650–C1655.
- Curran, M.E., I. Splawski, K.W. Timothy, G.M. Vincent, E.D. Green, and M.T. Keating. 1995. A molecular basis for cardiac arrhythmia: *HERG* mutations cause long QT syndrome. *Cell.* 80:795–803.
- DeCoursey, T.E., and S. Grinstein. 1998. Ion channels and carriers in leukocytes. In *Inflammation: Basic Principles and Clinical Correlates*. 3rd ed. J.I. Gallin, R. Snyderman, D.T. Fearon, B.F. Haynes, and C. Nathan, editors. Raven Press, New York. In press.
- DeCoursey, T.E., S.Y. Kim, M.R. Silver, and F.N. Quandt. 1996. III. Ion channel expression in PMA-differentiated human THP-1 macrophages. *J. Membr. Biol.* 152:141–157.
- del Rio-Hortega, P. 1932. Microglia. In *Cytology and Cellular Pathology of the Nervous System*. W. Penfield, editor. P.B. Hoeber, New York. 481–534.
- Eder, C., H.-G. Fischer, U. Hadding, and U. Heinemann. 1995a. Properties of voltage-gated currents of microglia developed using macrophage colony-stimulating factor. *Pflügers Arch.* 430:526–533.
- Eder, C., H.-G. Fischer, U. Hadding, and U. Heinemann. 1995b. Properties of voltage-gated potassium currents of microglia differentiated with granulocyte/macrophage colony-stimulating factor. *J. Membr. Biol.* 147:137–147.
- Eder, C., R. Klee, and U. Heinemann. 1997. Distinct soluble astrocytic factors induce expression of outward K⁺ currents and ramification of brain macrophages. *Neurosci. Lett.* 226:147–150.
- Faravelli, L., A. Arcangeli, M. Olivetto, and E. Wanke. 1996. A *HERG*-like K⁺ channel in rat F-11 DRG cell line: pharmacological identification and biophysical characterization. *J. Physiol. (Camb.)* 496:13–23.
- Fedoroff, S. 1995. Development of microglia. In *Neuroglia*. H. Kettenmann, and B.R. Ransom, editors. Oxford University Press, New York. 162–181.
- Fedoroff, S., C. Hao, I. Ahmed, and L.J. Guilbert. 1993. Paracrine and autocrine signalling in regulation of microglial survival. In *Biology and Pathology of Astrocyte–Neuron Interactions*. S. Fedoroff, B.H.J. Juurlink, and D. Doucette, editors. Plenum Publishing Corp., New York. 247–261.
- Fenwick, E.M., A. Marty, and E. Neher. 1982. A patch clamp study of bovine chromaffin cells and of their sensitivity to acetylcholine. *J. Physiol. (Camb.)* 331:577–597.
- Fernandez, J.M., A.P. Fox, and S. Krasne. 1984. Membrane patches and whole-cell membranes: a comparison of electrical properties in rat clonal pituitary (GH3) cells. *J. Physiol. (Camb.)* 356:565–585.
- Fischer, H.-G., C. Eder, U. Hadding, and U. Heinemann. 1995. Cytokine-dependent K⁺ channel profile of microglia at immunologically defined functional states. *Neuroscience*. 64:183–191.
- Gallin, E.K., and L.C. McKinney. 1988. Patch-clamp studies in human macrophages: single-channel and whole-cell characterization of two K⁺ conductances. *J. Membr. Biol.* 103:55–66.
- Gallin, E.K., and P.A. Sheehy. 1985. Differential expression of inward and outward potassium currents in the macrophage-like cell line J774.1. *J. Physiol. (Camb.)* 369:475–499.
- Giulian, D. 1997. Reactive microglia and ischemic injury. In *Primer on Cerebrovascular Disease*. K.M.A. Welch, L.R. Caplan, D.J. Reis, B.K. Siesjö, and B. Weir, editors. Academic Press, New York. 117–124.
- Harvey, R.D., and R.E. Ten Eick. 1988. Characterization of the inward-rectifying potassium current in cat ventricular myocytes. *J. Gen. Physiol.* 91:593–615.
- Hestrin, S. 1981. The interaction of potassium with the activation of anomalous rectification in frog muscle membrane. *J. Physiol. (Camb.)* 317:497–508.
- Hodgkin, A.L., and A.F. Huxley. 1952. The dual effect of membrane potential on sodium conductance in the giant axon of *Loligo*. *J. Physiol. (Camb.)* 116:497–506.
- Hu, Q., and Y.L. Shi. 1997. Characterization of an inward-rectifying potassium current in NG108-15 neuroblastoma×glioma cells. *Pflügers Arch.* 433:617–625.
- Illes, P., W. Nörenberg, and P.J. Gebicke-Haerter. 1996. Molecular mechanisms of microglial activation. B. Voltage- and purinoceptor-operated channels in microglia. *Neurochem. Int.* 29:13–24.
- Ilschner, S., C. Ohlemeyer, G. Gimpl, and H. Kettenmann. 1995. Modulation of potassium currents in cultured murine microglial cells by receptor activation and intracellular pathways. *Neuroscience*. 66:983–1000.
- Kettenmann, H., R. Banati, and W. Walz. 1993. Electrophysiological behavior of microglia. *Glia*. 7:93–101.
- Kettenmann, H., D. Hoppe, K. Gottmann, R. Banati, and G. Kreutzberg. 1990. Cultured microglial cells have a distinct pattern of membrane channels different from peritoneal macrophages. *J. Neurosci. Res.* 26:278–287.
- Korotzer, A.R., and C.W. Cotman. 1992. Voltage-gated currents expressed by rat microglia in culture. *Glia*. 6:81–88.
- Ling, E.-A., and W.-C. Wong. 1993. The origin and nature of ramified and amoeboid microglia: a historical review and current concepts. *Glia*. 7:9–18.
- Liu, S., R.L. Rasmusson, D.L. Campbell, S. Wang, and H.C. Strauss. 1996. Activation and inactivation kinetics of an E-4031-sensitive current from single ferret atrial myocytes. *Biophys. J.* 70:2704–2715.
- McKinney, L.C., and E.K. Gallin. 1988. Inwardly rectifying whole-cell and single-channel K currents in the murine macrophage cell line J774.1. *J. Membr. Biol.* 103:41–53.
- McKinney, L.C., and E.K. Gallin. 1990. Effect of adherence, cell morphology, and lipopolysaccharide on potassium conductance and passive membrane properties of murine macrophage J774.1 cells. *J. Membr. Biol.* 116:47–56.
- Nelson, D.J., B. Jow, and F. Jow. 1990. Whole cell currents in macrophages: I. Human monocyte-derived macrophages. *J. Membr. Biol.* 117:29–44.
- Nörenberg, W., K. Appel, J. Bauer, P.J. Gebicke-Haerter, and P. Illes. 1993. Expression of an outwardly rectifying K⁺ channel in rat microglia cultivated on Teflon. *Neurosci. Lett.* 160:69–72.
- Nörenberg, W., P.J. Gebicke-Haerter, and P. Illes. 1992. Inflammatory stimuli induce a new K⁺ outward current in cultured rat microglia. *Neurosci. Lett.* 147:171–174.

- Nörenberg, W., P.J. Gebicke-Haerter, and P. Illes. 1994. Voltage-dependent potassium channels in activated rat microglia. *J. Physiol. (Camb.)* 475:15–32.
- Pennefather, P.S., W. Zhou, and T.E. DeCoursey. 1998. Idiosyncratic gating of HERG-like K⁺ channels in microglia. *J. Gen. Physiol.* 111:795–805.
- Pennefather, P., C. Oliva, and N. Mulrine. 1992. Origin of the potassium and voltage dependence of the cardiac inwardly rectifying K-current (I_{K1}). *Biophys. J.* 61:448–462.
- Randriamampita, C., and A. Trautmann. 1987. Ionic channels in murine macrophages. *J. Cell Biol.* 105:761–769.
- Sanguinetti, M.C., C. Jiang, M.E. Curran, and M.T. Keating. 1995. A mechanistic link between an inherited and an acquired cardiac arrhythmia: *HERG* encodes the I_{Kr} potassium channel. *Cell* 81:299–307.
- Sanguinetti, M.C., and N.K. Jurkiewicz. 1990a. Two components of cardiac delayed rectifier K⁺ current: differential sensitivity to block by class III antiarrhythmic agents. *J. Gen. Physiol.* 96:195–215.
- Sanguinetti, M.C., and N.K. Jurkiewicz. 1990b. Lanthanum blocks a specific component of I_K and screens membrane surface charge in cardiac cells. *Am. J. Physiol.* 259:H1881–H1889.
- Schelper, R.L., and E.K. Adrian. 1986. Monocytes become macrophages: they do not become microglia: a light and electron microscopic autoradiographic study using 125-iododeoxyuridine. *J. Neuropathol. Exp. Neurol.* 45:1–19.
- Schlichter, L.C., G. Sakellaropoulos, B. Ballyk, P.S. Pennefather, and D.J. Phipps. 1996. Properties of K⁺ and Cl⁻ channels and their involvement in proliferation of rat microglial cells. *Glia* 17:225–236.
- Schönherr, R., and S.H. Heinemann. 1996. Molecular determinants for activation and inactivation of HERG, a human inward rectifier potassium channel. *J. Physiol. (Camb.)* 493:635–642.
- Shibasaki, T. 1987. Conductance and kinetics of delayed rectifier potassium channels in nodal cells of the rabbit heart. *J. Physiol. (Camb.)* 387:227–250.
- Sievers, J., J. Schmidtmyer, and R. Parwaresch. 1994. Blood monocytes and spleen macrophages differentiate into microglia-like cells when cultured on astrocytes. *Ann. Anat.* 176:45–51.
- Silver, M.R., and T.E. DeCoursey. 1990. Intrinsic gating of inward rectifier in bovine pulmonary artery endothelial cells in the presence or absence of internal Mg²⁺. *J. Gen. Physiol.* 96:109–133.
- Smith, P.L., T. Baukowitz, and G. Yellen. 1996. The inward rectification mechanism of the HERG cardiac potassium channel. *Nature* 379:833–836.
- Snyders, D.J., and A. Chaudhary. 1996. High affinity open channel block by dofetilide of *HERG* expressed in a human cell line. *Mol. Pharmacol.* 49:949–955.
- Spector, P.S., M.E. Curran, A. Zou, M.T. Keating, and M.C. Sanguinetti. 1996a. Fast inactivation causes rectification of the I_{Kr} channel. *J. Gen. Physiol.* 107:611–619.
- Spector, P.S., M.E. Curran, M.T. Keating, and M.C. Sanguinetti. 1996b. Class III antiarrhythmic drugs block HERG, a human cardiac delayed rectifier K⁺ channel. Open-channel block by methanesulfonanilides. *Circ. Res.* 78:499–503.
- Streit, W.J. 1990. An improved staining method for rat microglial cells using the lectin from *Griffonia simplicifolia* (GSA I-B₄). *J. Histochem. Cytochem.* 38:1683–1686.
- Streit, W.J., and C.A. Kincaid-Colton. 1995. The brain's immune system. *Sci. Am.* 273:54–61.
- Theele, D.P., and W.J. Streit. 1993. A chronicle of microglial ontogeny. *Glia* 7:5–8.
- Trudeau, M.C., J.W. Warmke, B. Ganetzky, and G.A. Robertson. 1995. HERG, a human inward rectifier in the voltage-gated potassium channel family. *Science* 269:92–95.
- Visentin, S., C. Agresti, M. Patrizio, and G. Levi. 1995. Ion channels in rat microglia and their different sensitivity to lipopolysaccharide and interferon- γ . *J. Neurosci. Res.* 42:439–451.
- Wang, S., M.J. Morales, S. Liu, H.C. Strauss, and R.L. Rasmusson. 1996. Time, voltage and ionic concentration dependence of h-erg expressed in *Xenopus* oocytes. *FEBS Lett.* 389:167–173.
- Wang, S., S. Liu, M.J. Morales, H.C. Strauss, and R.L. Rasmusson. 1997. A quantitative analysis of the activation and inactivation kinetics of *HERG* expressed in *Xenopus* oocytes. *J. Physiol. (Camb.)* 502:45–60.
- Warmke, J.W., and B. Ganetzky. 1994. A family of potassium channel genes related to *eag* in *Drosophila* and mammals. *Proc. Natl. Acad. Sci. USA* 91:3438–3442.
- Weinsberg, F., C.K. Bauer, and J.R. Schwarz. 1997. The class III antiarrhythmic agent E-4031 selectively blocks the inactivating inward-rectifying potassium current in rat anterior pituitary tumor cells (GH₃/B₆ cells). *Pflügers Arch.* 434:1–10.
- Wymore, R.S., G.A. Gintant, R.T. Wymore, J.E. Dixon, D. McKinnon, and I.S. Cohen. 1997. Tissue and species distribution of mRNA for the I_{Kr}-like K⁺ channel, *erg*. *Circ. Res.* 80:261–268.
- Yang, T., D.J. Snyders, and D.M. Roden. 1997. Rapid inactivation determines the rectification and [K⁺]_o dependence of the rapid component of the delayed rectifier K⁺ current in cardiac cells. *Circ. Res.* 80:782–789.
- Yang, T., M.S. Wathen, A. Felipe, M.M. Tamkun, D.J. Snyders, and D.M. Roden. 1994. K⁺ currents and K⁺ channel mRNA in cultured atrial cardiac myocytes (AT-1 cells). *Circ. Res.* 75:870–878.
- Yoo, A.S.J., J.G. McLarnon, R.L. Xu, Y.B. Lee, C. Krieger, and S.U. Kim. 1996. Effects of phorbol ester on intracellular Ca²⁺ and membrane currents in cultured human microglia. *Neurosci. Lett.* 218:37–40.
- Ypey, D.L., and D.E. Clapham. 1984. Development of a delayed outward-rectifying K conductance in cultured mouse peritoneal macrophages. *Proc. Natl. Acad. Sci. USA* 81:3083–3087.